ARTICLE

Synthesis and Luminescent Properties of Nano-scale $Y_2Si_2O_7$:Re^{3+} (Re=Eu, Tb) Phosphors via Sol-Gel Method

Yong Li[a,b], Bao-gui You[a], Wei Zhao[a], Wei-ping Zhang[a], Min Yin[a,b]*

a. Hefei National Laboratory for Physical Sciences at the Microscale, University of Science and Technology of China, Hefei 230026, China
b. Department of Physics, University of Science and Technology of China, Hefei 230026, China

(Dated: Received on November 18, 2007; Accepted on March 12, 2008)

By using metal nitrates as starting materials and citric acid as a complexing agent, $Y_2Si_2O_7$:Re^{3+} (Re=Eu, Tb) phosphors were prepared by a sol-gel method. X-ray diffraction was employed to characterize the resulting samples. The results of XRD indicate that the α-$Y_2Si_2O_7$ nanocrystal with size of 27 nm is obtained at 1000 °C and the doping ion content does not influence the structure. The excitation spectra in the UV and VUV ranges and the emission spectra of Re^{3+} doped samples were measured. The excitation spectra in the VUV range is due to absorption of host, that in the UV range is ascribed to absorption transitions from 4f to 5d state of the Tb^{3+} and the charge transfer in the $Eu^{3+}-O^{2-}$ bond. The spectral energy distribution of the Tb^{3+} emission depends strongly on the Tb^{3+} concentration. The dependence of photoluminescence intensity on Re^{3+} concentration is also discussed in detail. The fluorescent decay curves at room temperature were measured and analyzed.

Key words: Luminescence, Sol-gel, $Y_2Si_2O_7$, Rare earth

I. INTRODUCTION

Silicate-based phosphors have attracted much attention because of its excellent thermal and chemical stability, lower cost, and high luminescent efficiency [1,2]. Yttrium silicate is an important luminescent host material for various rare-earth activators [3]. Tm^{3+}-, Pr^{3+}-Er^{3+}- and Yb^{3+}-doped $Y_2Si_2O_5$ have been proposed as promising laser crystals [4-8]. The Tb^{3+}-activated $Y_2Si_2O_5$ has been widely studied in the application of displays and lamps because of its high luminescence efficiency and stability at the conditions of high irradiance with an electron beam [9-12]. The Ce^{3+}-doped $Y_2Si_2O_5$, which was discovered decades ago, is still one of the best low-voltage blue phosphors in field emission displays (FED) because of its excellent luminescence efficiency, color purity, and stability [13-18]. $Y_2Si_2O_5$:Eu^{3+} with its sharp emission in red was found to be a promising candidate phosphor for coherent time-domain optical memory (CTDOM) applications as well as high resolution displays [19-23]. Consequently, several preparation methods were aimed at the synthesis of luminescent nanosized $Y_2Si_2O_5$:Eu^{3+} in the form of fine powders [24,25] or films [26] by the sol-gel technique and by a metallorganic decomposition process.

For a long time the study on luminescent properties of rare earth-activated yttrium silicate was concentrated merely on yttrium orthosilicates; there are few reports on yttrium pyrosilicates. The binary disilicates, and specially the rare earth disicates, have been widely studied for their magnetic, electrical properties [27]. In particular, these materials exhibit an adequate behavior for luminescent applications as plasma displays, laser materials, and high-energy phosphors when doped with rare-earth elements. The luminescence of these phosphors is very efficient under both cathode ray and UV excitation [28,29]. Yttrium disilicate ($Y_2Si_2O_7$) is one of the most refractory silicates with a melting point of 1775 °C and is thus potentially useful as a high temperature structural ceramic. In the case of luminescence properties of rare earth doped $Y_2Si_2O_7$, only the luminescence of Ce^{3+} and Eu^{3+} has been studied [30,31].

The traditional method of synthesis for $Y_2Si_2O_7$ is to apply solid-state reaction between Y_2O_3 and SiO_2 at temperatures in the range 1200-1600 °C for the periods up to 100 h [32]. Recently, many advanced methods for preparing inorganic solid materials have been developed, one of which is sol-gel method. Compared with the conventional solid-state method, the sol-gel method is much simple, and has the advantages of easy stoichiometric control, good homogeneity through mixing the starting materials at the molecular level in solution, lower synthesis temperature and shorter heating time, and so on [33-36]. In this present work, Re^{3+}-doped (Re=Eu, Tb) yttrium pyrosilicates were prepared by using sol-gel method. The structural and spectroscopic characterization are reported. In particular, the effect of doping ion concentration upon the structure and luminescence properties was focused on. The amorphous and crystalline phases of the samples at the various thermal treatments were monitored through XRD. The concentration quenching phenomena are investigated. The luminescence properties at different concentrations are discussed.

*Author to whom correspondence should be addressed. E-mail: yinmin@ustc.edu.cn

II. EXPERIMENTS

Polycrystalline samples $Y_2Si_2O_7$:Re^{3+}(Re=Eu, Tb) with different concentrations were prepared by sol-gel method. The starting materials were Eu_2O_3 (4N), Tb_4O_7 (4N), Y_2O_3 (4N). The oxides were dissolved in dilute nitric acid separately to form corresponding nitrate solutions, then a stoichiometric amount of the above solutions were mixed. Then certain amounts of citric acid were added to the mixed nitrate solution. The $Si(OC_2H_5)_4$ was dissolved in C_2H_5OH, and then mixed with the nitrate solution. The mixture was stirred to achieve a uniform mixing, and ammonia or nitric acid was used to keep the pH of the resulting solution at about 2.0. After warming by water-bath at 70 °C for a period, the solution turned to a sticky transparent sol, and then to a gel. The gel was put into a furnace for pre-calcination at 450 °C for 2 h, then ground to powders, and finally was annealed at the required temperatures from 900 °C to 1000 °C for 2 h to obtain the phosphor samples. All the powders appear to be white color in body.

An X-ray diffractometer (MAC Science Co. Ltd MXP18AHF) with Cu Kα radiation was used for crystal phase identification and estimation of the crystallite size. The scan was performed in the 2θ range of 10°-70°. The emission and excitation spectra were measured at the VUV station of the National Synchrotron Radiation Laboratory (NSRL) in Hefei, China. The excitation spectra were corrected for the photo flux of the excitation beam using the excitation spectrum of sodium salicyate as standard. The integration time of 1 s and wavelength step of 1 nm were applied for all of spectrum measurements. The fourth-order harmonic of YAG:Nd laser (266 nm) was used as an excitation source for decay curves measurement. The luminescent decay profile was recorded by a Tektronix TDS3052B oscilloscope interfaced with a computer. All the spectra were performed at room temperature.

III. RESULTS AND DISCUSSION

A. Crystallization behaviors of the phosphors

The XRD patterns of $Y_2Si_2O_7$ by the sol-gel method with sintering at different temperatures between 900 and 1000 °C are presented in Fig.1(a). For the sample annealed at 900 °C, an obvious broadening diffraction peak located at 2θ=29.6° is observed, which is the characteristic peak for $Y_2Si_2O_7$. It can be seen the sample starts to crystallize at 900 °C. As annealing temperature is increased to 1000 °C, the diffraction pattern of the sample shows that all the peaks are indexes to the α-$Y_2Si_2O_7$ phase, which was confirmed by comparing with the diffraction data of JCPDS card No.21-1457, and no other crystalline phase can be detected. Further heat treatment leads to the enhancement in the α-$Y_2Si_2O_7$ diffraction peak and reduction in the full-

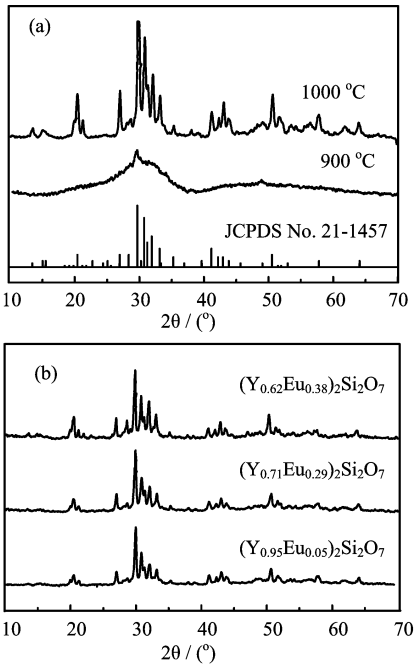

FIG. 1 (a) XRD patterns of $Y_2Si_2O_7$ prepared by sol-gel method annealed at 900 °C, 1000 °C for 2 h; (b) XRD patterns of $Y_2Si_2O_7$:Eu^{3+} with different Eu^{3+} content annealed at 1000 °C.

width at half-maximum due to the improvement of crystallinity and grain growth. The structure of rare-earth silicates has been intensively studied for a few decades due to both basic and applied interests. y, α, β, γ, and δ are the known polymorphs of $Y_2Si_2O_7$, which transform from one to another with increasing temperature [37]. Transition temperatures between the different $Y_2Si_2O_7$ polymorphs as well as temperature stability ranges vary considerably from one study to the others [38]. In this work, the phase transitions have shown a direct transformation from amorphous phase to α-$Y_2Si_2O_7$. The y-phase showes no stability field in this case. This is different from the results reported by Alba [39], which indicated that the y-$Y_2Si_2O_7$ polymorph is the stable phase at annealed temperature $T\leq$1000 °C. The α-type $Y_2Si_2O_7$ which is isotypic with α-$Ho_2Si_2O_7$ has triclinic structure with space group symmetry $P\bar{1}$, and it is built up of $[Si_3O_{10}]^{8-}$ groups plus additional $[SiO_4]^{4-}$ tetrahedra, whereas the other four types (y, β, γ, and δ) are generally built up of $[Si_2O_7]^{6-}$ units linked by cations [40,41].

The average crystallite size can be calculated by Scherrer's equation: D=0.89λ/Bcosθ, where λ, θ, and B are the wavelength of the X-ray, the diffraction angle and the corrected full width at half maximum of the diffraction peaks respectively, while 0.89 is a constant for spherical particles. The average crystallite for the sample annealed at 1000 °C is around 27 nm. The effect of doping concentration ($Y_2Si_2O_7$:$x$mol%Re^{3+}, 0<x<40) on the crystal phase of α-$Y_2Si_2O_7$ was inves-

DOI:10.1088/1674-0068/21/04/376-380

tigated. XRD results of $Y_2Si_2O_7$:Eu^{3+} powders containing various Eu^{3+} concentrations are presented in Fig.1(b). All of the peaks can be indexed to the α-$Y_2Si_2O_7$ phase, indicating that the doping ions do not form new phases in the synthesis process. The crystal structure of the $Y_2Si_2O_7$:Tb^{3+} powders with different concentration were also examined by XRD. The obtained spectra are not shown here. As mentioned previously, the $Y_2Si_2O_7$:Tb^{3+} powders with different concentration have the same structure.

B. Luminescence properties

Figure 2 shows the excitation and emission spectra of $Y_2Si_2O_7$:1mol%Tb^{3+} phosphor sintered at 1000 °C. The excitation spectrum consists of two broad bands: one broad band ranging from 130 nm to 185 nm is due to absorption of host, another one ranging from 185 nm to 250 nm with a maximum of 226 nm corresponds to the absorption transition of Tb^{3+} from $4f^8$ ground state to the excited $4f^75d^1$ state. The emission spectrum consists of a series of sharp lines in the region from 350 nm to 650 nm. The peaks at 378, 416, 436, and 458 nm can be attributed to $^5D_3$-^7F_J (J=6, 5, 4, 3) transitions of Tb^{3+}. The other four peaks at 487, 541, 589, and 622 nm are due to $^5D_4$-^7F_J (J=6, 5, 4, 3) transitions. The spectral energy distribution of Tb^{3+} emission depends strongly on Tb^{3+} concentration.

Figure 3 presents the emission spectra at different doping concentration of Tb^{3+}. At a low concentration (x=0.05), both the blue emission $^5D_3$-^7F_J and the green emission $^5D_4$-^7F_J are observed. With an increase of Tb^{3+} concentration, the blue emission is quenched gradually and disappears when the concentration is around 9mol%. The luminescence from $^5D_3$ level becomes weak and that from $^5D_4$ is enhanced, resulting in the emission color changing from white to green. The quenching of $^5D_3$ emission is due to the cross-relaxation process: $^5D_3+{}^7F_6 \rightarrow {}^5D_4+{}^7F_0$.

The relative integral intensity of blue emission $^5D_3$-^7F_J and green emission $^5D_4$-^7F_J as functions of Tb^{3+} concentration are illustrated in Fig.4. It is found that the intensity of both transitions increases at first with Tb^{3+} content increasing, and then decreases. The optimum concentration for the blue emission $^5D_3$-^7F_J and the green emission $^5D_4$-^7F_J is determined to be about 1mol% and 17mol%.

The phosphors of Eu^{3+}-doped material are found to exhibit a red emission under UV excitation (λ_{em}=240 nm). Figure 5 presents the emission spectra under 240 nm excitation. The emission spectra are described by the well-known $^5D_0$-^7F_J (J=0, 1, 2, 3, 4) line emissions of the Eu^{3+} with the strong emission J=2 at 611 nm ($^5D_0$-$^7F_2$). If a rare earth ion in the crystal lattice occupies a site with inversion symmetry, optical transitions between levels of the $4f^n$ configurations are strictly forbidden as electric-dipole transitions. They can only occur as magnetic-dipole transitions. If there is no inversion symmetry at the site of the rare earth ion, the uneven crystal field components can mix opposite-

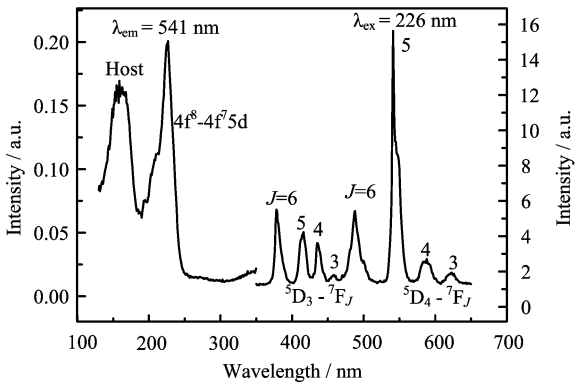

FIG. 2 Excitation and emission spectra of $Y_2Si_2O_7$:1mol%Tb^{3+}.

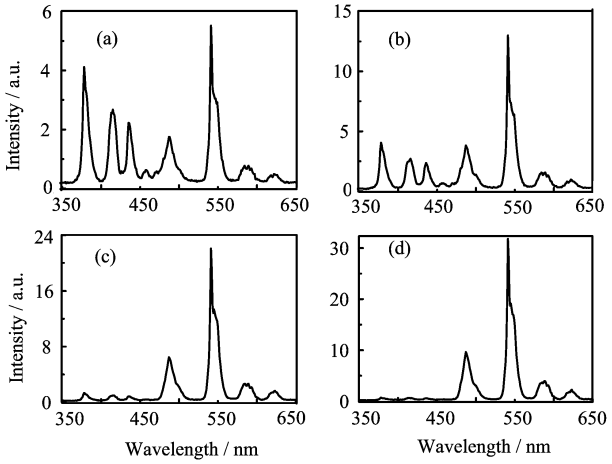

FIG. 3 The emission spectra of Tb^{3+}-doped $Y_2Si_2O_7$ under 226 nm excitation with different doping concentration of Tb^{3+}. (a) 0.5mol%, (b) 1mol%, (c) 3mol%, (d) 5mol%.

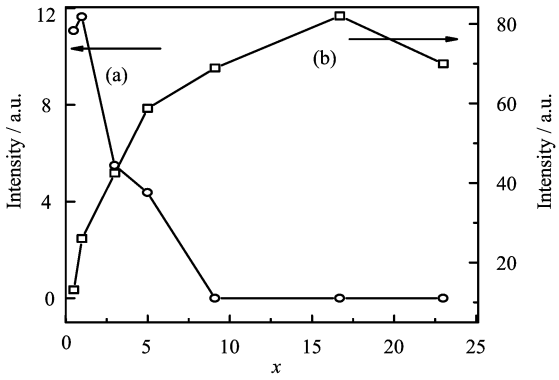

FIG. 4 The dependence of photoluminescence intensity on Tb^{3+} concentration in $Y_2Si_2O_7$:$x$mol%Tb^{3+} phosphors under 226 nm excitation. (a) $^5D_4$-^7F_J transition, (b) $^5D_3$-^7F_J transition.

DOI:10.1088/1674-0068/21/04/376-380

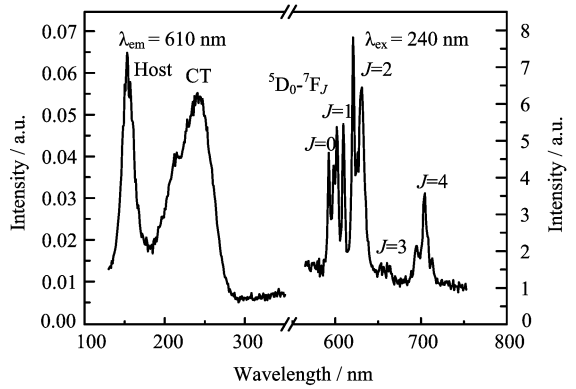

FIG. 5 Excitation and emission spectra of $Y_2Si_2O_7$:1mol%Eu^{3+}.

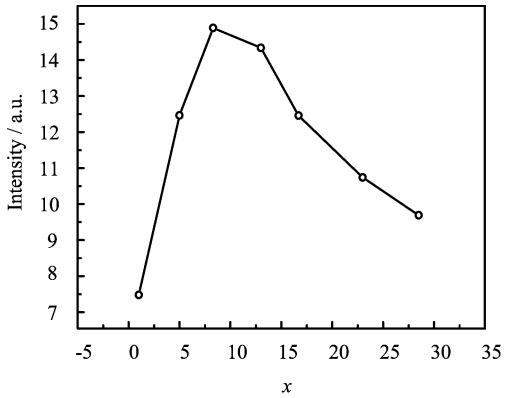

FIG. 6 Effects of Eu^{3+} content on integral intensity of the $^5D_0$-^7F_J emission of $Y_2Si_2O_7$:$x$mol%Eu^{3+} phosphors under 240 nm excitation.

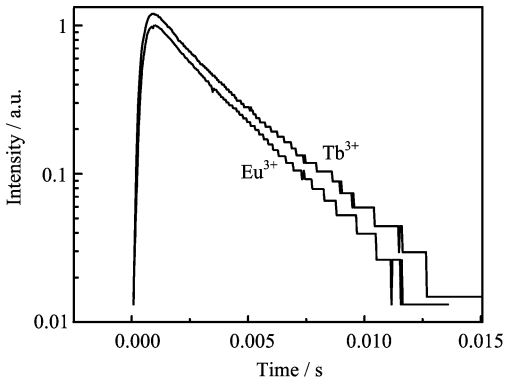

FIG. 7 Fluorescence decay curves of $^5D_4$ levels in Tb^{3+} for $Y_2Si_2O_7$:3mol%Tb^{3+} and $^5D_0$ levels in Eu^{3+} for $Y_2Si_2O_7$:5mol%Eu^{3+}, λ_{ex}=266 nm.

parity states into the $4f^n$-configurational levels. The electric-dipole transitions are now no longer strictly forbidden and appear as lines in the spectra, and the $^5D_0$-$^7F_2$ transition can be observed, which is hypersensitive to ligand environment. In the emission spectra of $Y_2Si_2O_7$:1mol%Eu^{3+}, the electric dipole $^5D_0$-$^7F_2$ transition around 611 nm is stronger than that of the magnetic dipole $^5D_0$-$^7F_1$ transition around 590 nm. This indicates that Eu^{3+} occupy the non-inversion symmetric sites. It can be found that only emissions from the level $^5D_0$ were observed, indicating that the emissions from $^5D_2$ and $^5D_1$ are quenched due to a cross-relaxation process, which is enabled by the closely matched energy difference between $^5D_1$ ($^5D_2$) and $^5D_0$ levels and the $^7F_3$ ($^7F_5$) and $^7F_0$ levels [42]. Besides the cross-relaxation process, the luminescence from ^5D_J levels can be quenched also by high-energy lattice phonons leading to the multiphonon relaxation process, especially in silicate compounds [42].

C. Electric-dipole transition

In the excitation spectrum, as shown in Fig.5, the host absorption band centered at 153 nm is also observed. The band peak at 240 nm is due to the charge-transfer in the $Eu^{3+}-O^{2-}$ bond, which corresponds to an electron transfer from an oxygen 2p orbit to an empty 4f orbital of europium ion is predominant.

The dependence of integral intensity ($^5D_0$-^7F_J) on Eu^{3+} concentration is shown in Fig.6. It can be seen that the emission intensity increases with increasing Eu^{3+} content and reaches the maximum value at 8mol% Eu^{3+} doping, and then descends at higher contents indicating the concentration quenching.

The fluorescent decay curves of 611 nm emission for $Y_2Si_2O_7$:5mol%Eu^{3+} and 542 nm emission for $Y_2Si_2O_7$:3mol%Tb^{3+} were measured under 266 nm excitation at room temperature, as shown in Fig.7. All the decay curves rise first and then fall. The appearance of the rise time indicates the presence of a slow relaxation feeding the emitting level. When Tb^{3+} ions are excited by UV (266 nm) wavelengths, Tb^{3+} ions absorb the excitation energy, and the transitions from the ground state to the excited state (5d) occur, after which Tb^{3+} ions relax to the $^5D_4$ state. The $^5D_4$ state can be populated by two processes, a non-radiative multi-phonon relaxation from the 5d levels or a cross-relaxation involving the $^5D_3$-$^5D_4$ and $^7F_6$-$^7F_0$ transitions, as mentioned previously. That is the reason that the decay curve exhibits a rise time after pulse excitation (266 nm). After the relaxation process, the green emission of Tb^{3+} occurs. The decay curves can be well fitted into single exponential function as $I=A\exp(-t/\tau)$, a lifetime τ value of 2.89 ms is obtained for (541 nm) emission of Tb^{3+}. As for Eu^{3+} ions under 266 nm excitation, they are excited to the charge transfer state first, and then are relaxed to $^5D_0$ state by the multi-phonon relaxation, and maybe a cross-relaxation involving $^5D_1$ ($^5D_2$)-$^5D_0$ levels and the $^7F_3$ ($^7F_5$) -$^7F_0$ transitions. A lifetime τ value of 2.74 ms is obtained for (611 nm) emission of Eu^{3+}.

DOI:10.1088/1674-0068/21/04/376-380

IV. CONCLUSION

Nano-crystalline $Y_2Si_2O_7$:Re^{3+}(Re=Eu, Tb) phosphors were prepared by sol-gel method with citric acid as additive in precursor solutions. XRD patterns indicate that the α-type structure of $Y_2Si_2O_7$ is obtained at 1000 °C, and the doping ions do not influence the structure. The excitation spectra in the VUV range is due to absorption of host, and that in UV range is ascribed to absorption transitions from 4f to 5d state of Tb^{3+} ion and the charge-transfer in the $Eu^{3+}-O^{2-}$ bond. The spectral energy distribution of Tb^{3+} emission depends strongly on Tb^{3+} concentration. For low Tb^{3+} content, $Y_2Si_2O_7$:5mol%Eu^{3+} material exhibits blue and green emissions arising from $^5D_3$ and $^5D_4$ levels. An increase in the concentration leads to the extinction of that originating from $^5D_3$ by a cross-relaxation mechanism, giving rise to strong emission from $^5D_4$. The optimum concentration for $^5D_3$-^7F_J and $^5D_4$-^7F_J of Tb^{3+} is determined to be 1mol% and 20mol%, respectively. The decays were measured and can be fitted by single exponential procedure. The lifetimes obtained by fitting the curves are 2.89 and 2.74 ms, respectively.

V. ACKNOWLEDGMENTS

This work was supported by the National Natural Science Foundation of China (No.50332050 and No.10774140), the Funds for International Cooperation and Exchange of the NSFC (No.50711120504), the Specialized Research Fund for the Doctoral Program of Higher Education (No.20060358054), and the Special Foundation for Talents of Anhui Province, China (No.2077Z021)

[1] Z. G. Xiao, United States Patent 6.093.346.
[2] C. S. Shi, Y. B. Fu, B. Liu, G. B. Zhang, Y. H. Chen, Z. M. Qi, and X. X. Luo, J. Lumin. **122-123**, 11 (2007).
[3] J. Shmulovich, G. W. Berkstresser, C. D. Brandle, and A. Valentino, J. Electrochem. Soc. **135**, 3141 (1988).
[4] E. Bielejec, E. Kisel, and A. Silversmith, J. Lumin. **72-74**, 62 (1997).
[5] Y. V. Malyukin, A. A. Masalov, and P. N. Zhmurin, Phys. Lett. A **316**, 147 (2003).
[6] C. H. Hu, C. L. Sun, J. F. Li, Z. S. Li, H. Z. Zhang, and Z. K. Jiang, Chem. Phys. **325**, 563 (2006).
[7] S. Campos, A. Denoyer, S. Jandl, B. Viana, D. Vivien, P. Loiseau, and B. Ferrand, J. Phys. Condens. Matter **16**, 4579 (2004).
[8] A. Novoselov, H. Ogino, A. Yoshikawa, M. Nikl, J. Pejchal, A. Beitlerova, and T. Fukuda, Opt. Mater. **29**, 1381 (2007).
[9] Q. Su, J. Lin, H. Zhang, and S. Wang, Mater. Res. Bull. **31**, 189 (1996).
[10] H. S. Kang, Y. C. Kang, H. D. Park, and Y. G. Shul, Appl. Phys. A **80**, 347 (2005).
[11] H. J. Lee, S. K. Hong, D. S. Jung, S. H. Ju, H. Y. Koo, and Y. C. Kang, Ceram. Int. **32**, 865 (2006).
[12] Z. H. Zhang, Y. H. Wang, Y. Hao, and W. J. Liu, J. Alloys and Compd. Lett. **433**, L12 (2007).
[13] M. Mitsunaga, R. Yano, and N. Uesugi, Opt. Lett. **16**, 1890 (1991).
[14] H. Suzuki, T. A. Tombrello, C. L. Melcher, and J.S. Schweitzer, Nucl. Instrum. Meth. A **320**, 263 (1992).
[15] P. J. Marsh, J. Silver, A. Vecht, and A. Newport, J. Lumin. **97**, 229 (2002).
[16] Q. Y. Zhang, K. Pita, W. Ye, W. X. Que, and C. H. Kam, Chem. Phys. Lett. **356**, 161 (2002).
[17] H. Jiao, L. Q. Wei, N. Zhang, M. Zhong, and X. P. Jing, J. Euro. Ceram. Soc. **27**, 185 (2007).
[18] E. Coetsee, J. J. Terblans, and H. C. Swart, J. Lumin. **126**, 37 (2007).
[19] X. A. Shen and R. Kachru, J. Opt. Soc. Am. B **591**, 11 (1994).
[20] M. Yin, W. Zhang, S. Xia, and J. C. Krupa, J. Lumin. **68**, 335 (1996).
[21] M. Yin, W. Zhang, L. Lou, S. Xia, and J. C. Krupa, Physica B **254**, 141 (1998).
[22] X. Qin, Y. G. Ju, S. Bernhard, and N. Yao, Mater. Res. Bull. **42**, 1440 (2007).
[23] W. Zhang, P. Xie, C. Duan, K. Yan, M. Yin, L. Lou, S. Xia, and J. C. Krupa, Chem. Phys. Lett. **292**, 133 (1998).
[24] M. Yin, C. Duan, K. Yan, L. Lou, S. Xia, and J. C. Krupa, J. Appl. Phys. **86**, 3751 (1999).
[25] Y. Liu, C. N. Xu, H. Chen, and H. J. Tateyama, J. Luimin. **97**, 135 (2002).
[26] Q. Y. Zhang, K. Pita, W. Ye, W. Ye, W. X. Que, and C. H. Kam, Chem. Phys. Lett. **356**, 161 (2002).
[27] J. Felsche, Struct. Bond. **13**, 100 (1973).
[28] Y. Y. Choi, K. S. Sohn, H. D. Park, and S. Y. Choi, J. Mater. Res. **16**, 881 (2001).
[29] M. Diaz, C. Pecharroman, F. del Monte, J. Sanz, J. E. Iglesias, J. S. Moya, C. Yamagata, and S. Mello-Castanho, Chem. Mater. **17**, 1774 (2005).
[30] N. Karar and H. Chander, J. Phys. D Appl. Phys. **38**, 3580 (2005).
[31] P. L. Zhou, X. B. Yu, L. Z. Yang, S. P. Yang, and W. J. Gao, J. Lumin. **124**, 241 (2007).
[32] A. N. Christensen, R. G. Hazell, and A. W. Hewat, Acta. Chem. Scand. **51**, 37 (1997).
[33] M. Q. Wang, X. P. Fan, and G. H. Xiong, J. Phys. Chem. Solids **56**, 859 (1995).
[34] M. Yu, J. Lin, Y. H. Zhou, M. L. Pang, X. M. Han, and S. B. Wang, Thin Solid Films **444**, 245 (2003).
[35] A. Bao, H. Yang, C. Y. Tao, Y. Zhang, and L. L. Han, J. Lumin. **128**, 60 (2008).
[36] C. C. Lin, K. M. Lin, and Y. Y. Li, J. Lumin. **126**, 795 (2007).
[37] J. Feslche, Struct. Bond. **13**, 99 (1973).
[38] G. Tzvetkov and N. Minkova, J. Mater. Sci. Lett. **20**, 1273 (2001).
[39] A. I. Becerro, M. Naranjo, M. D. Alba, and J. M. Trillo, J. Mater. Chem. **13**, 1835 (2003).
[40] J. Felsche, Struct. Bond. **13**, 100 (1973).
[41] J. Parmentier, P. R. Bodart, L. Audoin, G. Massouras, D. P. Thompson, R. K. Harris, P. Goursat, and J. L. Besson, J. Solid State Chem. **149**, 16 (2000).
[42] G. Blasse and B. C. Grabmaier, *Luminescent Materials*, Berlin: Springer-Verlag, (1994).

DOI:10.1088/1674-0068/21/04/376-380